

MiR-193-3p attenuates the vascular remodeling in pulmonary arterial hypertension by targeting PAK4

Zhenhua Wu^{1,*}, Jie Geng^{2,*}, Yujuan Qi¹, Jian Li¹, Yaobang Bai¹ and Zhigang Guo³

¹Department of Cardiac Surgery, ICU, Tianjin Chest Hospital, Tianjin, China; ²Department of Cardiac Surgery, CICU, Tianjin Chest Hospital, Tianjin, China;

³Department of Cardiac Surgery, Tianjin Chest Hospital, Tianjin, China

Abstract

Pulmonary arterial hypertension (PAH) is a progressive pulmonary vascular disease associated with dysfunction of pulmonary artery endothelial cells and pulmonary artery smooth muscle cells (PASMCs). To explore the potential mechanism of miR-193-3p in pulmonary arterial hypertension, human PASMCs and rats were respectively stimulated by hypoxia and monocrotaline to establish PAH model in vivo and in vitro. The expressions of miR-193-3p and p21-activated protein kinase 4 (PAK4) in the lung samples of PAH patients and paired healthy samples from the healthy subjects in PHA cells and rats were detected by quantitative reverse transcriptase-PCR. Morphological changes in lung tissues were determined using hematoxylin and eosin staining. Right ventricular systolic pressure (RVSP) and ratio of right ventricle to left ventricle plus septum (RV/LV p S) were measured. The binding relationship between miR-193-3p and PAK4 was analyzed by TargetScan and verified by luciferase reporter assay. Cell viability, apoptosis, and migration were detected by 3-(4, 5-Dimethylthiazol-2-yl)-2,5-diphenyltetrazolium bromide (MTT) flow cytometry, and wound-healing assays, respectively. The protein expressions of PAK4, proliferating cell nuclear antigen (PCNA), P21, p-AKT, and AKT in vivo or in vitro were determined by Western blot. In this study, we found that in pulmonary arterial hypertension, miR-193-3p expression was downregulated and PAK4 expression was up-regulated. MiR-193-3p directly targeted PAK4 and negatively regulated its expression. Hypoxia condition promoted cell proliferation, migration, and inhibited apoptosis accompanied with increased expressions of PCNA and p-AKT/AKT and decreased expression of P21 in PASMCs. MiR-193-3p overexpression attenuated the effects of hypoxia on PASMCs via downregulating PAK4. Monocrotaline treatment increased p-AKT/AKT and decreased P21 expression and caused pulmonary vascular remodeling in the model rats. MiR-193-3p overexpression attenuated pulmonary vascular remodeling, decreased p-AKT/AKT, and increased P21 levels via downregulating PAK4 in monocrotaline-induced rats. The results in this study demonstrated that upregulation of miR-193-3p reduced cell proliferation, migration, and apoptosis of PAH in vitro and pulmonary vascular remodeling in PAH in vivo through downregulating PAK4.

Keywords

MiR-193-3p, PAK4, pulmonary arterial hypertension, pulmonary vascular remodeling

Date received: 18 June 2020; accepted: 29 October 2020

Pulmonary Circulation 2020; 10(4) 1–12

DOI: 10.1177/2045894020974919

Introduction

Pulmonary arterial hypertension (PAH), which is a type of pulmonary hypertension that affects pulmonary vasculature primarily,¹ is a progressive pulmonary vascular disease related to high morbidity and mortality.² The application of novel targeted drugs (e.g. endothelin receptor blockers, prostaglandin analogs, phosphodiesterase-5 inhibitors) increased the five-year survival rate of PAH patients to 55% and even 70%, but long-term effect is still unfavorable.^{3,4} PAH is characterized by a persistent elevation of pulmonary arterial pressure, partially due to uncontrolled

vascular remodeling.⁵ Attenuating vascular remodeling has been considered as a strategy of managing PAH, but currently we still lack effective treatment targeting vascular remodeling.⁶ The molecular mechanisms underlying

*These authors contributed equally to this work.

Corresponding author:

Zhigang Guo, Department of Cardiac Surgery, Tianjin Chest Hospital, No. 261, South Taierzhuang Road, Jinnan District, Tianjin 300222, China.
Email: guozhigang_guozg@163.com



Creative Commons Non Commercial CC BY-NC: This article is distributed under the terms of the Creative Commons Attribution-NonCommercial 4.0 License (<https://creativecommons.org/licenses/by-nc/4.0/>) which permits non-commercial use, reproduction and distribution of the work without further permission provided the original work is attributed as specified on the SAGE and Open Access pages (<https://us.sagepub.com/en-us/nam/open-access-at-sage>).

© The Author(s) 2020
Article reuse guidelines:
sagepub.com/journals-permissions
journals.sagepub.com/home/pul



vascular remodeling remains largely elusive, which require further investigation on the potential molecular mechanism of vascular remodeling in PAH and development of new effective treatments for PAH management.

MicroRNAs (miRNAs) are a series of small endogenous non-coding RNAs that serve as elemental modulators of numerous genes through binding to the 3'-untranslated regions (3'-UTR) of mRNAs, leading to the suppression of translation and degradation of the transcripts.⁷ Dysregulation of miRNAs participates in the regulation of cardiovascular diseases such as neovascularization, vasoconstriction regulation, hypertension, and atherosclerosis.⁸ It has been demonstrated that multiple miRNAs exhibit abnormal expressions in the development of PAH, and are involved in PAH progression and pulmonary arterial remodeling by regulating key factors in some downstream signaling pathways.⁹ MiRNAs are reported to regulate pulmonary artery smooth muscle cells (PASMCs) phenotypes and pulmonary remodeling under hypoxia.¹⁰ For example, upregulation of miRNA-17-5p facilitates the hypoxia-induced proliferation of human PASMCs by targeting p21 and phosphatase and tensin homologue (PTEN)¹¹; similarly, miR-34a facilitates the proliferation of human PASMCs through modulation of platelet-derived growth factor receptor alpha (PDGFRA) under hypoxia.¹² Upregulation of miR-214 contributes to the development of vascular remodeling in PAH caused by hypoxia via regulating cyclin L2 (CCNL2).¹³ Downregulated miR-193 functions critically in the lungs from PAH rats.¹⁴ Sharma et al.¹⁵ suggested that miR-193-3p (miR-193) participates in the pathological process of PAH and attenuates pulmonary vascular remodeling; however, the potential molecular mechanism of miR-193-3p in pulmonary vascular remodeling of PAH remained to be fully explored.

In this study, we aimed to determine the expression of miR-193-3p and its corresponding downstream target gene as well as their interaction in pulmonary vascular remodeling of PAH *in vitro* and *in vivo*, hoping to provide new biomarkers for PAH therapy.

Materials and method

Ethics statement

All the patients had signed informed consent, and agreed that their tissues and plasma would be used for any experimental work involving humans. The clinical trial program had been reviewed and approved by the Ethics Committee of Tianjin Chest Hospital (TCH20180211015).

In compliance with the guidelines of the China Council on Animal Care and Use, all experiments for animals were performed in Tianjin Chest Hospital and approved by the Committee of Experimental Animals of Tianjin Chest Hospital (TCH20190325066). Efforts were devoted to minimize their sufferings.

Patients and clinical sample collection

Before operation, 10 lung tissue samples of PAH patients (six females and four males, average age of 36.1 ± 2.2 years, mean PAH was 86 ± 16 mm Hg) who received lung transplantation and 10 paired healthy control samples (seven females and three males, average age of 34.8 ± 2.0 years) from the unused donor control subjects were collected at Tianjin Chest Hospital from March 2018 to March 2019. All the PAH patients did not have a history of local or systemic treatment. The tissue samples were immediately transferred into chilled oxygenated Krebs solution (pH 7.4) containing 116.6 mM NaCl, 21.9 mM NaHCO₃, 11 mM D-glucose, 1.2 mM MgSO₄, 4.2 mM KCl, 1.6 mM NaH₂PO₄, and 2.5 mM CaCl₂.

Cell culture and treatment

Human PASMCs were obtained from Cell Applications (352-05a, San Diego, CA, USA) and maintained in SmGM-2TM smooth muscle growth medium-2 (CC-3182, Lonza, USA, www.lonza.com/) with 5% fetal bovine serum (FBS). For normoxic treatment, the cells were cultured with 21% O₂, 5% CO₂, and balanced N₂; for hypoxic induction, the cells were cultured with 2% O₂, 5% CO₂, and balanced N₂ for the indicated time intervals, following a previous report.¹⁶

Cell transfection

MiR-193-3p mimic (5'-AACUGGCCUACAAAGUCCCA GU-3') and corresponding mimic control (5'-CGCA GGUCAAGUGGCCGACUUA-3') were purchased from GenePharma. Modified pcDNA3.1 vector containing PAK4 sequence was commercially constructed by RiboBio (Guangzhou, China). Empty pcDNA3.1 vector (V79020, ThermoFisher, USA) was used as a negative control (NC). The PASMCs were transfected with miRNA mimics and pcDNAs using Lipofectamine 3000 Reagent (L3000015, Thermo Fisher Scientific, Inc.), according to the manufacturers' instruction.

Luciferase reporter assay

TargetScan V7.2 (www.targetscan.org/vert_72/) was used to explore targets of miR-193-3p. The 3'-UTR segment of PAK4 (5'-CCCCGCCCCACTGAGGCCAGTA-3') with putative complementary binding sites of miR-193-3p was ligated into pmirGLO vector (E1330, Promega, USA) for the construction of PAK4 wild-type (PAK4-WT) luciferase reporter vector. The 3'-UTR segment of PAK4 (5'-CCCCGCCCCACTGAATGGCCGA-3') with putative binding site of mutant (MUT) miR-193-3p was ligated into the pmirGLO vector by RiboBio for the construction of PAK4-WT. The PASMCs were transfected with PAK4-WT, or PAK4-MUT and MiR-193-3p mimic, or mimic control. Following 48-h transfection, the luciferase activity was determined by the dual-luciferase reporter assay system (E1910, Promega).

Cell viability

Cell viability of PSMCs was detected using MTT kit (11465007001, Sigma-Aldrich, Shanghai, China) following manufacturer's protocol. In short, before the addition of MTT solution (5 mg/mL), the treated cells (1×10^3 cell/well) were inoculated into a 96-well plate for 24 h. Next, the cells were cultured for 4 h at 37°C. The absorbance at 490 nm was determined by a microplate reader (Tecan, Switzerland). After 4-h incubation at 37°C, the cells were further added with 150 μ L of dimethylsulfoxide. Microplate reader (Tecan, Switzerland) was then employed to measure the absorbance at 570 nm.

Immunofluorescence assay

To determine the proliferation of the PSMCs, after transfected under hypoxic conditions for 48 h, the cells were fixed with 4% paraformaldehyde at room temperature for 15 min, and incubated overnight with anti-PCNA antibody at 4°C. Alexa Fluor 488 conjugated mouse IgG was used as a secondary antibody. Images were taken using a laser scanning confocal microscope (Leica, Heidelberg, Germany). 2-(4-Amidinophenyl)-6-indolecarbamide dihydrochloride (DAPI) was used to counterstain nuclei and the nuclei of cell positive for PCNA was calculated.

Flow cytometry assay

To determine the apoptosis rate of the PSMCs, Annexin V-FITC and propidium iodide (PI) double staining was conducted using an Annexin V-FITC Apoptosis Detection Kit (CA1020, Solarbio, China). Briefly, the treated cells were collected, washed twice with phosphate buffer solution (PBS), and resuspended at 1×10^6 cells/mL in 100 μ L of binding buffer. Then, the cells were treated with Annexin V-FITC and PI for 15 min at 37°C in the dark and blended with 400 μ L of binding buffer. Flow cytometer AccuriTM C6 (BD Biosciences) was performed within 1 h. The results were analyzed by the Cell Quest software 3.3 (Becton-Dickinson).

Wounding-healing migration assay

Cell migration of PSMCs was determined by wound-healing assay. In short, the transfected cells (4×10^5 cells/well) were plated into in the complete medium in six-well plates. Following 8-h culture, the PSMCs were starved in SmGM-2 medium with 0.2% FBS overnight. Next, a scratch was performed on the cell monolayer using a 10 μ L tip and the previous medium was replaced by complete medium. The images were photographed at 0 h under a 100 \times inverted microscope (Ts2r-FL, Nikon, Japan). Then the cells were exposed to hypoxia or normoxia for 24 h, and images were captured by the same method. Cell migration rate was determined by measuring the reduced width of scratch on the PSMCs.

Animal model and groups

Thirty adult male Sprague Dawley rats (body weight 160–200 g) were purchased from the Slack Laboratory Animal based in Shanghai. A PAH rat model was induced by monocrotaline (MCT). The rats were randomly divided into five groups ($n=6$ /group) as follows: (1) Sham; (2) MCT; (3) MCT + agomiR – NC + NC; (4) MCT + agomiR-193-3p + NC; and (5) MCT + agomiR-193-3p + PAK4. The sham group was treated with 0.9% normal saline via intraperitoneal injection, while other groups were treated with 1% MCT (pH 7.4, 60 mg/kg). At week 4, severe PAH was observed in the all the groups except Sham group.

Recombinant adenovirus containing PAK4 (AdPAK4) or a green fluorescent protein (GFP)-only virus control (AdControl) was obtained from GenePharma (Shanghai, China). GFP-only virus control was a NC for AdPAK4. AgomiR-miR-193-3p and control agomiR (agomiR-NC) were purchased from RiboBio. To determine the effects of PAK4 and miR-193-3p in vivo, the PAH rats were nebulized with 50 μ L agomiR-miR-193-3p (20 μ mol/L) or/and 50 μ L adenovirus (1.5×10^8 pfu) once a week for two weeks, as previously reported.¹⁶

Hemodynamic measurements

Hemodynamic parameters were obtained: A heparinized pressure catheter (Millar Instruments, Houston, TX) was inserted into the right ventricle of rats through the right ventricle. Right ventricular systolic pressure (RVSP) was assessed using a physiological data acquisition system (LabChart 7.0; AD Instruments, Australia). The ratio of right ventricle to left ventricle plus septum (RV/LV+S) was used as an indicator of right ventricular hypertrophy (RVH). The pressure was recorded within 2 min and analyzed using Powerlab Pro software (AD Instruments, Germany).

Hematoxylin and eosin staining

Pulmonary artery tissues of rats were immediately collected after sacrifice and fixed with 10% paraformaldehyde for at least two days at room temperature, and then decalcified in 0.5 M EDTA (pH = 8.0) and embedded in paraffin. Sections were cut into 3- μ m thick, mounted on glass slides, stained with an hematoxylin and eosin (H&E) staining kit (G1120, Solarbio, China) and visualized using a 100 \times inverted microscope (Ts2r-FL, Nikon, Japan). To quantify the wall thickness (WT%) and the vessel area percentage (WA%) to evaluate the pulmonary vascular remodeling and the external and internal area: WT% = (external diameter – internal diameter)/external diameter \times 100%. WA% = (external area – internal area)/external area \times 100%.

Western blot

Total protein was isolated from the cultured PSMCs and collected from pulmonary artery tissues using a radio immunoprecipitation assay buffer (RIPA) buffer (P0013, Beyotime, China), and the content was quantified by BCA protein assay kit (PC0020, Solarbio). The proteins were separated using 10% SDS-PAGE and blotted onto polyvinylidene difluoride (PVDF) membranes (FFP32, Beyotime). Protein markers (PR1910 (11-180kDa) and PR1920 (11-245KD)) were purchased from Beijing Solarbio Science & Technology Co., Ltd. After blocking the membranes using 5% bovine serum albumin (BSA) for 2 h 37°C, the membranes were first treated with primary antibodies (presented in Table 1) overnight at 4°C and then treated with corresponding secondary antibodies (ab205719 or ab205718, Abcam, USA). Finally, the membranes were subjected to ECL solution (P0018FS, Beyotime), and specific bands were visualized by a Quantity One 1-D Analysis Software (Bio-Rad). The protein expression was normalized to that of β -actin. Primary antibodies used for western blots were listed in Table 1.

Quantitative reverse transcription polymerase chain reaction

Total RNA was separated from the lung samples and cultured cells by applying TRIzol® (Invitrogen; Thermo Fisher Scientific, Inc.), and then quantified using a NanoDrop spectrophotometer (Thermo Fisher Scientific, Inc.). TaqMan™ MicroRNA Reverse Transcription Kit (4366596, Applied Biosystems; Thermo Fisher Scientific, Inc.) and TaqMan MicroRNA assay (4427975, Applied Biosystems) were applied to perform quantitative reverse transcription polymerase chain reaction (qRT-PCR) for determining miR-193-3p expression. U6 was an endogenous control. Reverse transcription-PCR kit (RR036B, Takara) and TB Green PCR reagent (RR430A, Takara) were used to perform qRT-PCR for determining PAK4 expression in an Applied Biosystems 7300 Real-Time PCR system. β -actin was an internal control for PAK4. The relative expression of PAK4 was calculated by the $2^{-\Delta\Delta Ct}$ method.¹⁷ The primers (shown in Table 2) were obtained from Sangon Biotech (Shanghai, China).

Table 1. List of primary antibodies used for western blots.

Protein	Antibody	Catalog number	Company	Antibody dilution
PAK4	Rabbit	PA5-69540	Thermo Fisher Scientific, Inc.	1:1000
PCNA	Rabbit anti-PCNA antibody	ab92552	Abcam	1:1000
p21	Rabbit anti-p21 antibody	ab109199	Abcam	1:1000
p-AKT	Rabbit anti-AKT (phospho T308) antibody	ab38449	Abcam	1:1000
AKT	Rabbit anti-pan-AKT antibody	ab8805	Abcam	1:500
β -actin	Mouse anti-beta actin antibody	ab8226	Abcam	1:1000

Data analysis

Data were presented as the means \pm SD. Statistical analyses were conducted with SPSS version 13.0 software (SPSS, Chicago, IL, USA). Two-group comparison was performed with the Student's *t* test, while comparisons among multiple groups were conducted by one-way ANOVA followed by Bonferroni's post hoc test. Differences were considered as significance when $p < 0.05$.

Results

The expressions of miR-193-3p and PAK4 in the lung tissues from PAH patients and their binding relationship

The expression of miR-193-3p was observed to be markedly decreased in PAH patients compared with healthy groups (Fig. 1a, $p < 0.001$), while that of PAK4 was increased in PAH patients (Fig. 1b, $p < 0.001$). We also explored the relationship between miR-193-3p and PAK4 on TargetScan website and found that miR-193-3p had a binding site with PAK4 (Fig. 1c). The results of dual-luciferase report assay further showed that luciferase activity of miR-193-3p mimic + PAK4-WT group was significantly reduced as compared with Mimic control group (Fig. 1d, $p < 0.001$), but did not change obviously in miR-193-3p mimic + PAK4-MUT group (Fig. 1d). The data suggested that miR-193-3p directly targeted PAK4 in PSMCs.

Table 2. Primer sequences used for quantitative reverse transcription polymerase chain reaction (qRT-PCR).

Genes	Primer sequences (5'-3')
miR-193-3p	
Forward	TGGCCTACAAAGTCCCAGTG
Reverse	TGTCGTGGAGTCGGCAATTG
PAK4	
Forward	TCCCCCTGAGCCATTGTG
Reverse	ACCTGTCTCCCCATCCA
β -actin	
Forward	CATCTCGCCATGCTATTA
Reverse	AAGGTGGAGTCCTAAAGC
U6	
Forward	CTCGCTTCGGCAGCACA
Reverse	AACGCTTCACGAATTTGCGT

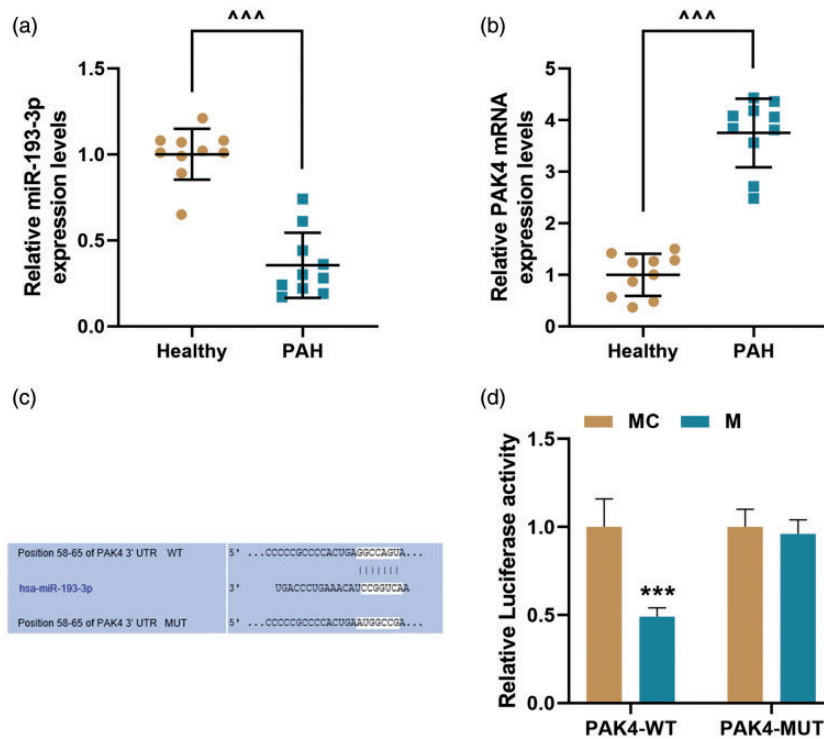


Fig. 1. The expressions of miR-193-3p and PAK4 in the lung tissues from human with PAH and their binding relationship ($n = 10$ /each group). (a) and (b) qRT-PCR detected the miR-193-3p expression (a) and PAK4 mRNA expression (b) in PAH and corresponding healthy groups. (c) TargetScan predicted the binding sites between miR-193-3p and PAK4. (d) Dual-luciferase report assay confirmed the binding relationship between miR-193-3p and PAK4. The experiment was repeated three times. ^{***} $p < 0.001$ vs. healthy; ^{***} $p < 0.001$ vs. MC. Data were presented as the means \pm SD.

PAH: pulmonary arterial hypertension.

The expressions of miR-193-3p and PAK4 and their interaction in hypoxia-induced PASCs

The HPASCs were subjected to hypoxia for 0, 3, 6, 12, 24, and 48 h. The results from qRT-PCR showed that compared with normal group (normoxia treatment), miR-193-3p expression was markedly decreased, especially at 24 h (Fig. 2a, $p < 0.05$ or $p < 0.001$). The mRNA expression of BMPR2 was obviously increased in the hypoxia-induced PASCs in a time-dependent manner (Fig. 2b, $p < 0.05$, $p < 0.01$, or $p < 0.001$). In hypoxia induction experiment, miR-193-3p expression was the lowest after hypoxia exposure for 24 h, therefore 24 h of hypoxia exposure was used for further experiments. In addition, miR-193-3p expression was markedly decreased in the hypoxia-induced PASCs (Fig. 2c, $p < 0.001$), but was partially increased by miR-193-3p mimic (Fig. 2c, $p < 0.001$). PAK4 expression was significantly increased in the hypoxia-induced PASCs (Fig. 2d, $p < 0.001$) but was partially reduced by miR-193-3p mimic (Fig. 2d, $p < 0.001$). However, the inhibitory effect of miR-193-3p mimic on PAK4 expression was partially reversed by PAK4 transfection (Fig. 2d, $p < 0.001$).

MiR-193-3p overexpression attenuated hypoxia-induced phenotypes and related-molecule expressions in the PASCs through inhibiting PAK4 expression

The viability of PASCs (Fig. 2e, $p < 0.001$) was significantly increased by hypoxia treatment, but was greatly reduced by miR-193-3p overexpression (Fig. 2e, $p < 0.001$). The inhibitory effect of miR-193-3p overexpression on the cell viability was significantly reversed by PAK4 overexpression (Fig. 2e, $p < 0.01$). Hypoxia treatment notably reduced apoptosis of PASCs (Fig. 3a and b, $p < 0.001$), which was obviously promoted by miR-193-3p overexpression (Fig. 3a and b, $p < 0.001$). However, the promoting effect of miR-193-3p overexpression on apoptosis was greatly inhibited by PAK4 overexpression (Fig. 3a and b, $p < 0.001$). Hypoxia treatment significantly facilitated the migration of PASCs (Fig. 3c and d, $p < 0.001$), which was significantly reversed by miR-193-3p overexpression (Fig. 3c and d, $p < 0.001$). Moreover, the inhibitory effect of miR-193-3p overexpression on the cell migration was noticeably reversed by PAK4 overexpression (Fig. 3c and d, $p < 0.01$). Immunofluorescence assay showed that hypoxia treatment significantly promoted the expressions of proliferation

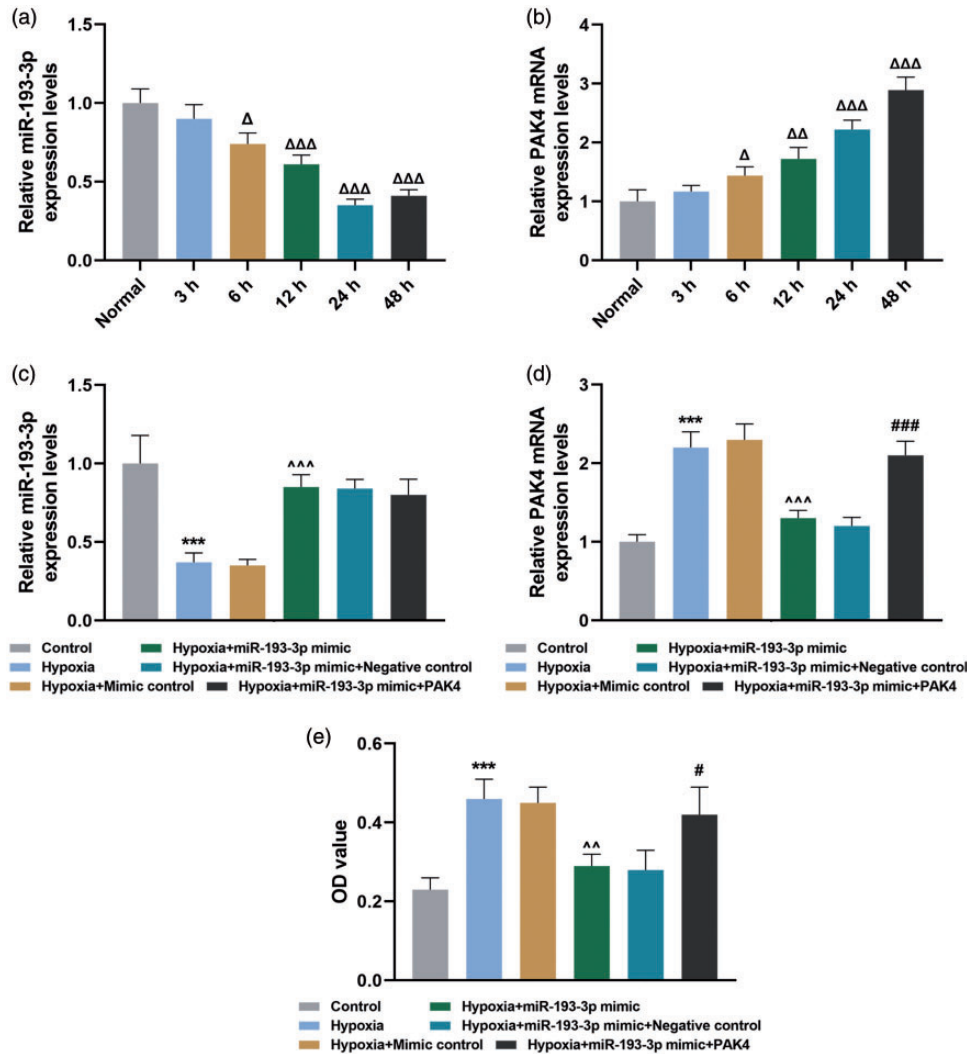


Fig. 2. The expressions of miR-193-3p and PAK4 and their interaction in hypoxia-induced PASMCs. (a) and (b) PASMCs were exposed to hypoxia for different times (0, 3, 6, 12, 24, and 48 h), followed by qRT-PCR assay on miR-193-3p expression (a) and PAK4 mRNA expression (b). (c)–(e) PASMCs were divided into control, hypoxia, hypoxia + mimic control, hypoxia + miR-193-3p mimic, hypoxia + miR-193-3p mimic + negative control, hypoxia + miR-193-3p mimic + PAK4 groups, followed by the detection of miR-193-3p expression by qRT-PCR analysis (a), PAK4 mRNA expression by qRT-PCR analysis (d), and cell proliferation ability by MTT assay (e). The experiment was repeated three times. $\Delta p < 0.05$ or $\Delta\Delta\Delta p < 0.001$ vs. normal; $*** p < 0.001$ vs. control; $^{***} p < 0.001$ vs. hypoxia; $^{##} p < 0.01$ or $^{####} p < 0.001$ vs. hypoxia + miR-193-3p mimic + negative control. Data were presented as the means \pm SD.

marker PCNA, which were reversed by miR-193-3p overexpression, and the effects of miR-193-3p overexpression on PCNA was significantly reversed by PAK4 overexpression (Fig. 4a and b). The Western blot experiment further verified this trend, hypoxia treatment significantly promoted the expressions of proliferation marker PCNA (Fig. 4c and d, $p < 0.001$) and phosphorylation of AKT (Fig. 4c–f, $p < 0.001$), inhibited P21 expression (Fig. 4c and d, $p < 0.001$), which were all greatly reversed by miR-193-3p overexpression (Fig. 4c–f, $p < 0.001$). However, the effects of miR-193-3p overexpression on PCNA, P21, and phosphorylation of AKT were significantly reversed by PAK4 overexpression (Fig. 4c–f, $p < 0.001$).

MiR-193-3p attenuated pulmonary vascular remodeling in the PAH rats through inhibiting PAK4 expression

MCT treatment significantly inhibited the expression of miR-193-3p (Fig. 5a, $p < 0.001$), which was markedly increased by agomiR-miR-193-3p (Fig. 5a, $p < 0.001$). Additionally, MCT treatment obviously promoted the mRNA and protein expressions of PAK4 (Fig. 5b–d, $p < 0.001$), which were significantly reversed by agomiR-miR-193-3p (Fig. 5b–d, $p < 0.001$). Moreover, the inhibitory effects of agomiR-miR-193-3p on the mRNA and protein expressions of PAK4 were markedly reversed by PAK4 overexpression (Fig. 5b–d, $p < 0.001$). Furthermore, rats in

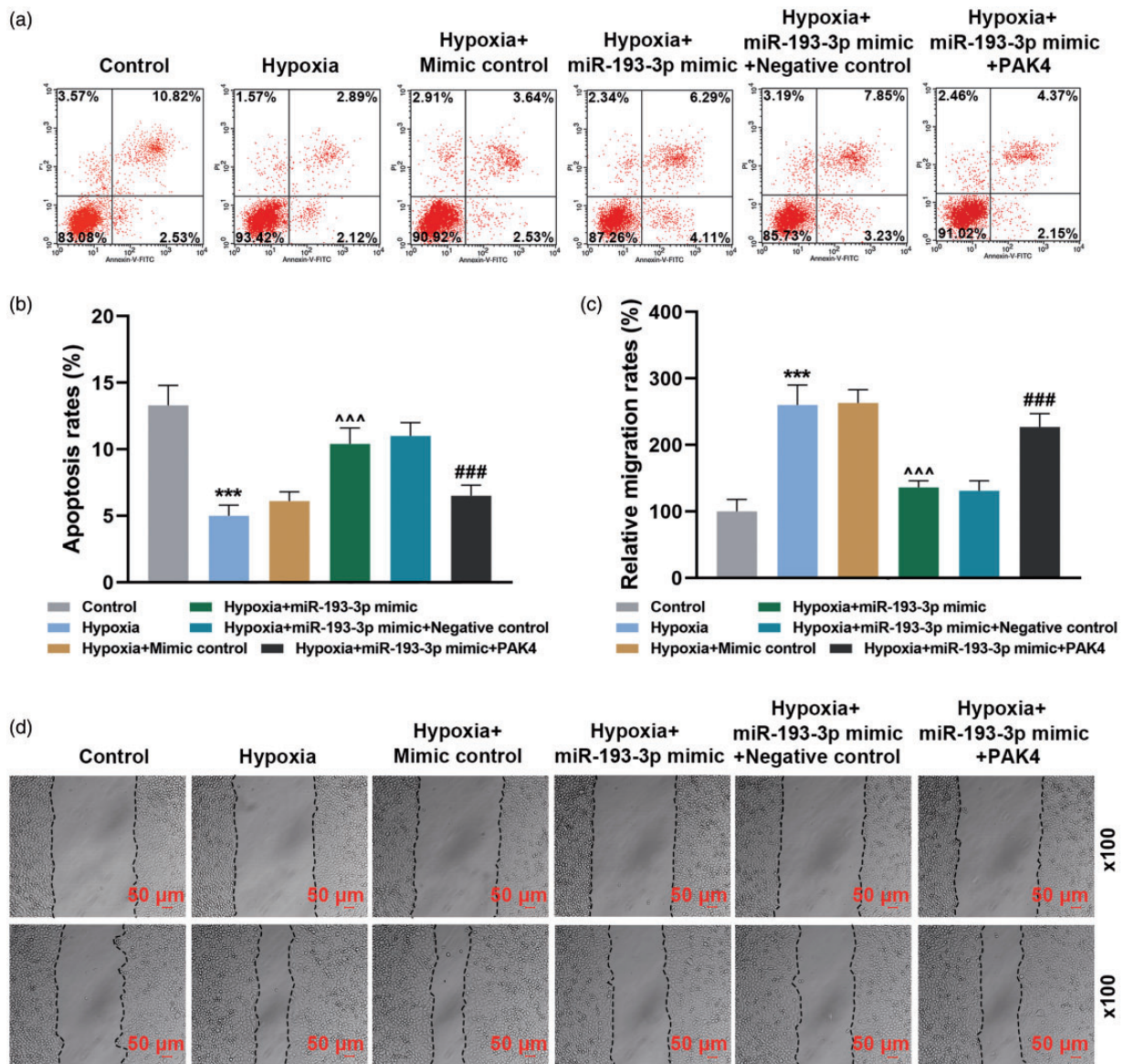


Fig. 3. MiR-193-3p overexpression attenuated hypoxia-induced phenotypes in PSMCs through inhibiting PAK4 expression. (a)–(d) PSMCs were divided into control, hypoxia, hypoxia + mimic control, hypoxia + miR-193-3p mimic, hypoxia + miR-193-3p mimic + negative control, hypoxia + miR-193-3p mimic + PAK4 groups, followed by the detection of apoptosis by flow cytometry analysis (a) and (b), and cell migration by wound-healing migration assay (c) and (d). The experiment was repeated three times. ^{*}*p* < 0.001 vs. control; ^{^^^}*p* < 0.001 vs. hypoxia; ^{###}*p* < 0.001 vs. hypoxia + miR-193-3p mimic + negative control. Data were presented as the means ± SD.

MCT group had a significant increase in RVSP compared with the sham group, which were significantly reversed by agomiR-miR-193-3p, and the inhibitory effects of agomiR-miR-193-3p on the RVSP were markedly reversed by PAK4 overexpression (Fig. 5e, *p* < 0.001). The ratio of RV/LV + S showed the same trend between groups (Fig. 5f, *p* < 0.001).

As shown in Fig. 6a, H&E staining showed severe pulmonary hemorrhage, pulmonary vascular remodeling, and pulmonary fibrosis in the MCT group as compared with Sham group, but such conditions in the MCT group were noticeably attenuated by miR-193-3p overexpression. However, the positive effect of miR-193-3p overexpression

was effectively reversed by PAK4 overexpression. WT% and WA% of the pulmonary arteries were significantly higher in MCT group, miR-193-3p overexpression significantly reversed this trend, and PAK4 overexpression markedly reversed the effect of agomiR-miR-193-3p (Fig. 6b and c, *p* < 0.001). In addition, the results from Western blot showed that MCT treatment significantly suppressed the expression of P21 (Fig. 6d–e, *p* < 0.001), and promoted the phosphorylation of AKT (Fig. 6d–f, *p* < 0.001). Following MCT treatment, miR-193-3p overexpression significantly promoted P21 expression (Fig. 6d–e, *p* < 0.001) and suppressed phosphorylation of AKT (Fig. 6d–f, *p* < 0.001). The effect of miR-193-3p overexpression was

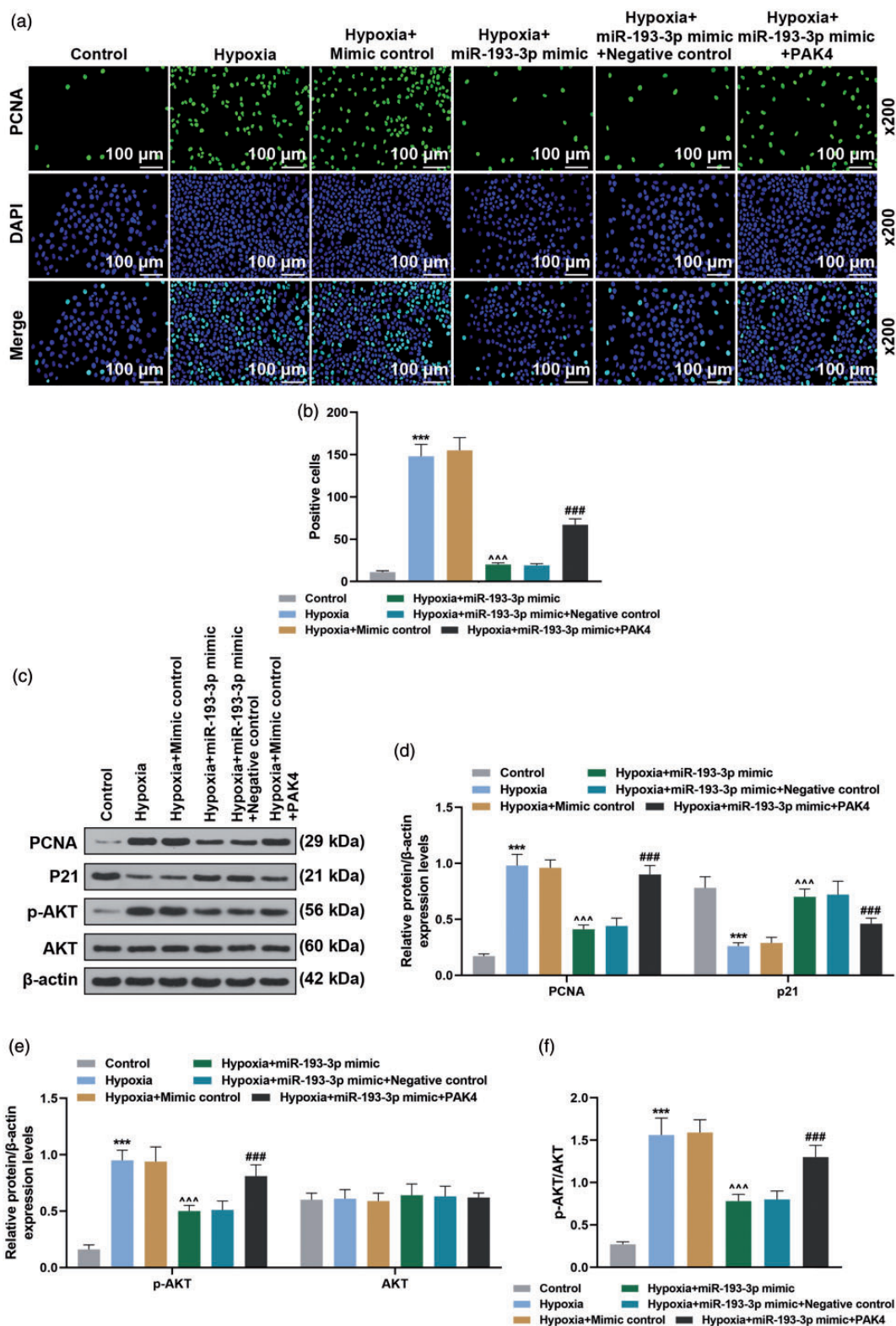


Fig. 4. MiR-193-3p overexpression regulated molecular expressions involved in hypoxia-induced PAH in PASMCS through inhibiting PAK4 expression. (a) and (b) PASMCS were divided into control, hypoxia, hypoxia + mimic control, hypoxia + miR-193-3p mimic, hypoxia + miR-193-3p mimic + negative control, hypoxia + miR-193-3p mimic + PAK4 groups, followed by the detection of PCNA by immunofluorescence, PCNA positive cells were counted. (c)–(e) The detection of protein expressions of p-AKT, AKT, PCNA, and p21 by Western blot. (f) A ratio of p-AKT to total AKT protein (p-AKT/AKT). The experiment was repeated three times. β -actin was used as internal control. ^{***} $p < 0.001$ vs. control; ^{^^^} $p < 0.001$ vs. hypoxia; ^{###} $p < 0.001$ vs. hypoxia + miR-193-3p mimic + negative control. Data were presented as the means \pm SD. p-AKT: phosphorylated AKT.

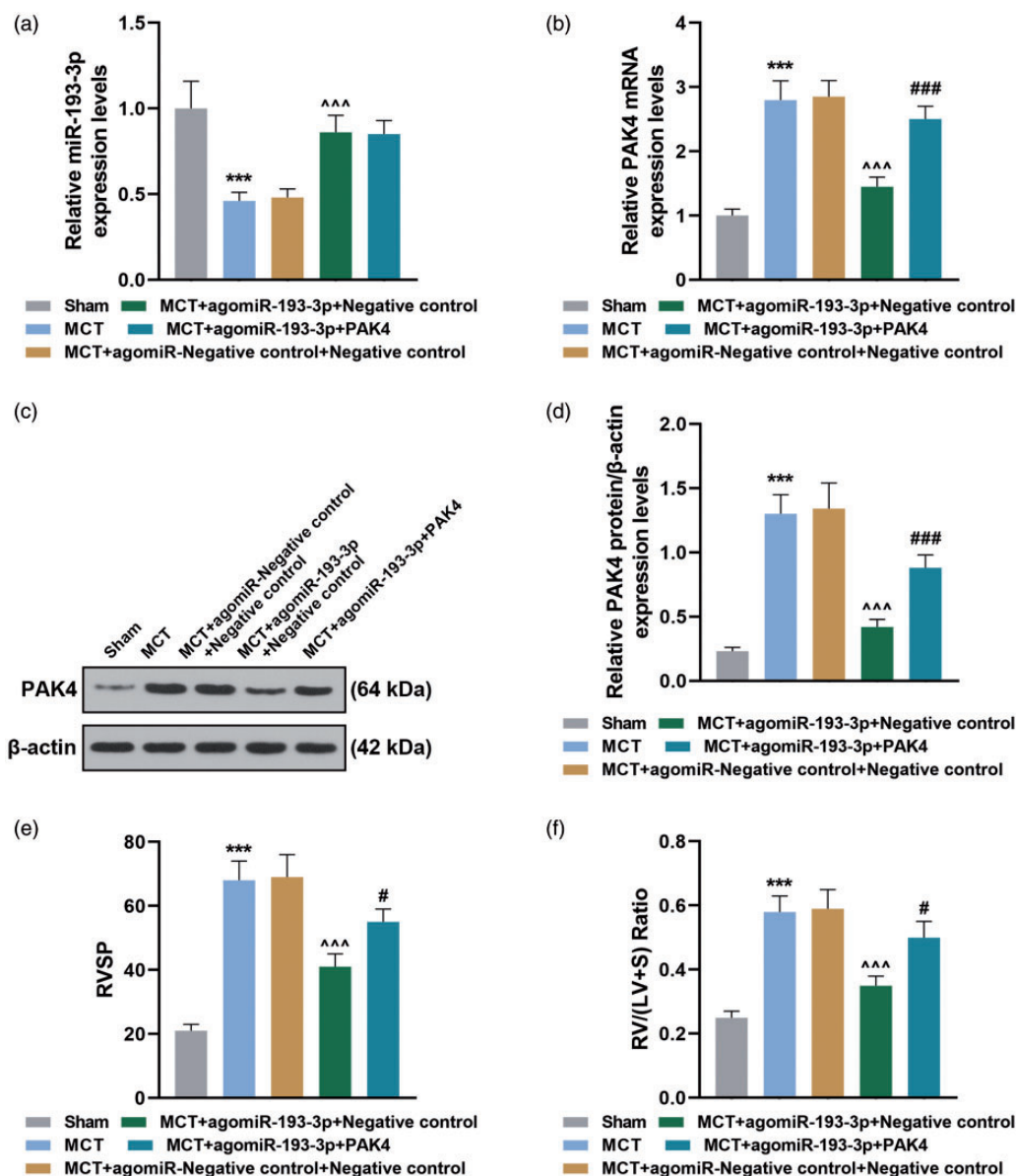


Fig. 5. MiR-193-3p overexpression inhibited PAK4 expression in PAH rats ($n=6$ /each group). The rats were divided into Sham, MCT, MCT + agomiR – negative control + negative control, MCT + agomiR-193-3p + negative control, MCT + agomiR-193-3p + PAK4 groups, following by the detection of expression of miR-193-3p by qRT-PCR analysis (a), PAK4 mRNA expression by qRT-PCR analysis (b), PAK4 protein expression by Western blot analysis (c) and (d). Right ventricular systolic pressure (RVSP) and ratio of right ventricle to left ventricle plus septum (RV/LV+S) were measured (e) and (f). β -actin was used as internal control. *** $p < 0.001$ vs. Sham; ^^^ $p < 0.001$ vs. MCT + agomiR – negative control + negative control; ##### $p < 0.001$ vs. MCT + agomiR-193-3p + PAK4.

Data were presented as the means \pm SD.

MCT: monocrotaline.

partially reversed by PAK4 overexpression (Fig. 6d–f, $p < 0.01$ or $p < 0.001$).

Discussion

PAK4 is normally low-expressed in multiple normal adult tissues,¹⁸ and its overexpression has been found in multiple cancers.^{19–21} Jian et al.²² reported that miR-193-3p is significantly overexpressed in both gastric cell lines and human

gastric tumors. Similarly, the present study found that miR-193-3p was downregulated in lung tissues of PAH patients, hypoxia-induced PSMCs, and the lung tissues of MCT-induced rats, whereas PAK4 resulted in opposite results. Thus, remarkably downregulated miR-193-3p in PAH should be further explored.

A new cancer-like concept has been proposed for PAH because the pathogenesis of PAH is similar to cancers, such as excessive cell proliferation and apoptosis inhibition.²³

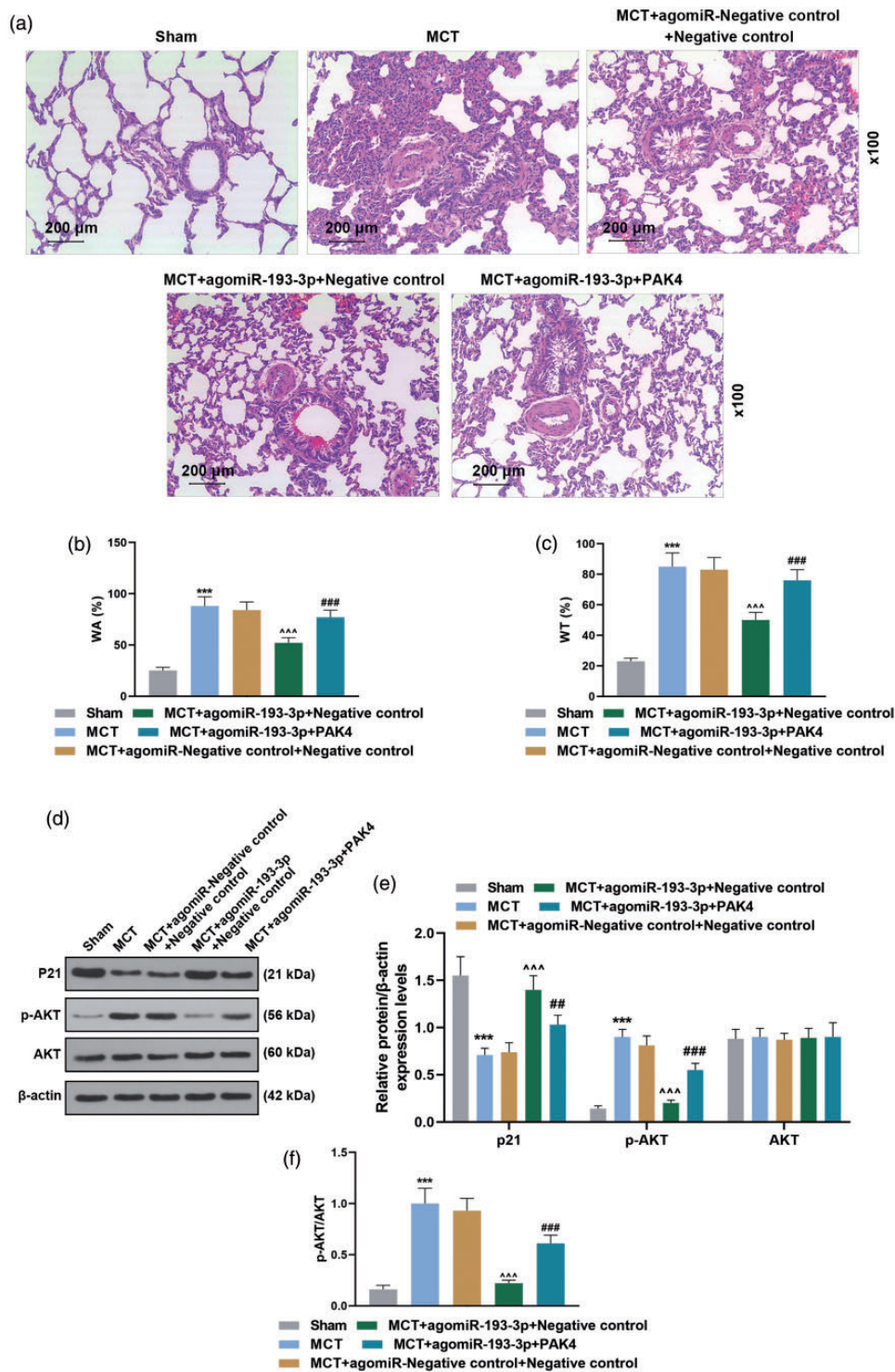


Fig. 6. MiR-193-3p attenuated pulmonary vascular remodeling in PAH rats through inhibiting PAK4 expression ($n = 6$ /each group). (a) Results of H&E staining of rat lung tissues in Sham, MCT, MCT + agomiR – negative control + negative control, MCT + agomiR-193-3p + negative control, MCT + agomiR-193-3p + PAK4 groups. (b) and (c) The wall thickness (WT%) and the vessel area percentage (WA%) were measured. (d)–(f) Western blot detected the protein expressions of p21, p-AKT, and AKT in Sham, MCT, MCT + agomiR – negative control + negative control, MCT + agomiR-193-3p + negative control, MCT + agomiR-193-3p + PAK4 groups. β -actin was used as internal control. *** $p < 0.001$ vs. Sham; ^{^^^} $p < 0.001$ vs. MCT + agomiR – negative control + negative control; ^{####} $p < 0.001$ vs. MCT + agomiR-193-3p+PAK4. Data were presented as the means \pm SD.

MCT: monocrotaline; p-AKT: phosphorylated AKT.

Increasing reports demonstrated that multiple miRNAs, such as miR-485²⁴ and miR-342,²⁵ regulate the development of cancer cells through targeting PAK4. The present study reported the association between miR-193-3p and PAK4 in PAH. We found that miR-193-3p carried a binding site with PAK4 using TargetScan V7.2, and the prediction was confirmed by dual-luciferase reporter assay. Moreover, miR-193-3p overexpression negatively regulated PAK4 expression under hypoxia. However, the regulatory roles of miR-193-3p and PAK4 in PAH phenotype remained unclear. It has been demonstrated that miRNAs play key parts in PAH pathogenesis, and can act as biomarkers and new therapeutic targets for PAH.²⁶ Tang et al.²⁷ demonstrated that miR-143-5p facilitates proliferation and migration of PSMCs in hypoxia by regulating Hypoxia-inducible factor-1 α (HIF-1 α). Zhao et al.²⁸ indicated that upregulation of miR-593-5p greatly suppresses the proliferation and migration of PSMCs through regulating polo-like kinase 1 (PLK1). Yue et al.²⁹ showed that miR-143 and miR-145 facilitate proliferation and migration of PSMCs via modulating ABCA1 expression under hypoxic condition. Similarly, we found that miR-193-3p overexpression inhibited cell proliferation and migration, provoked apoptosis of PSMCs in hypoxia through inhibiting PAK4 expression, pointing to the regulatory role of miR-193-3p and PAK4 in PAH phenotype. We then further explored the roles of miR-193-3p and PAK4 in PAH and the potential molecular mechanisms.

p21 is a cyclin-dependent kinase inhibitor that facilitates cell cycle arrest in response to various stimuli.³⁰ AKT plays a key role in modulating tumor cell survival and cell cycle progression.³¹ Previous study revealed that PAK4 plays a critical role in the initiation of cell cycle by modulating p21.³² Investigation by Yuan et al. showed that upregulation of PAK4 in vascular smooth muscle cells significantly suppresses p21 expression, enhances AKT activation, and further regulates cell cycle development and cell proliferation.³³ A previous report indicated that PAK4 is modulated by miRNA-433 and subsequently inhibits AKT signaling, thereby regulating the proliferation of hepatocellular carcinoma cells.³⁴ Moreover, the upregulation of miR-342 has been found to inhibit PAK4 expression, subsequently inactivates the AKT and ERK pathways in glioma, thus inhibiting the cell proliferation, invasion, and apoptosis resistance of glioma.²⁵ Similarly, in this study, we observed that miR-193-3p overexpression suppressed the expression of proliferation marker PCNA, AKT activation, and promoted p21 expression, which were all partially reversed by PAK4 overexpression in PSMCs under hypoxic condition. The present data suggested that miR-193-3p inhibited the proliferation of PSMCs by mediating cell cycle progression through targeting PAK4 via regulating p21 expression and AKT activation, and such a process was accompanied with decreased expression of PCNA. However, further research is required to study whether the effects of AKT activation and the expressions of

p21 and PCNA on the miR-193-3p targeting PAK4 in affecting the proliferation, migration, and vascular remodeling of PAH PSMCs is independent. The data from PAH rats caused by MCT also showed the same results to in vitro results in this study. In addition, the results from H&E staining assay showed that miR-193-3p overexpression attenuated lung vascular remodeling in rats injected with MCT through inhibiting PAK4 expression. It is known that the primary cellular mechanism underlying vascular remodeling is reflected by excessive proliferation and migration of PSMCs.²³ Thus, the current findings suggested that miR-193-3p attenuated the vascular remodeling in PAH by inhibiting PAK4 expression. Other researchers¹¹ have shown that miR-17-5p plays a part in PAH and the proliferation of PSMCs by regulating p21. A latest report³⁵ indicated that miR-182-3p can regulate pulmonary hypertension vascular remodeling and proliferation of PSMCs through KLF4/p21-dependent mechanism, which is consistent with our findings. However, based on the complex occurrence and development of diseases, whether there is an interaction network between miR-193-3p and other miRNAs such as miR-182-3p and miR-17-5p in PAH vascular remodeling should be further explored by future studies.

Taken together, in PAH, miR-193-3p was downregulated and PAK4 was up-regulated. MiR-193-3p suppressed PAK4 expression in PAH in vitro and in vivo. MiR-193-3p attenuated the proliferation, migration, and apoptosis resistance of PSMCs induced by hypoxia and vascular remodeling in the rats induced by MCT through targeting PAK4 to regulate Akt signaling, the p21 and PCNA. These findings demonstrated that miR-193-3p attenuated vascular remodeling in PAH by targeting PAK4 and may serve as a promising therapeutic target for the therapy of PAH. However, miRNAs-based treatments should be confirmed by conducting clinical experiments.

Author contributions

Substantial contributions to conception and design: Z.W. and J.G. Data acquisition, data analysis, and interpretation: Y.Q., J.L., Y. B., and Z.G.

Drafting the article or critically revising it for important intellectual content: Z.W. and J.G.

Final approval of the version to be published: all authors.

Agreement to be accountable for all aspects of the work in ensuring that questions related to the accuracy or integrity of the work are appropriately investigated and resolved: all authors.

Conflict of interest

The author(s) declare that there is no conflict of interest.

Ethics approval and consent to participate

All procedures performed in this study involving human participants were in accordance with the ethical standards of the institutional and/or national research committee and with the 1964 Helsinki declaration and its later amendments or comparable ethical standards.

Funding

The author(s) disclosed receipt of the following financial support for the research, authorship, and/or publication of this article: This work was supported by the Fund of Tianjin Chest Hospital (2018XKZ16).

References

- Thenappan T, Ormiston ML, Ryan JJ, et al. Pulmonary arterial hypertension: pathogenesis and clinical management. *BMJ* 2018; 360: j5492.
- Baillie TJ, Sidharta S, Steele PM, et al. Noninvasive assessment of cardiopulmonary reserve: toward early detection of pulmonary vascular disease. *Am J Respir Crit Care Med* 2017; 195: 398–401.
- Liu QQ and Jing ZC. The limits of oral therapy in pulmonary arterial hypertension management. *Ther Clin Risk Manag* 2015; 11: 1731–1741.
- Liu A, Li Z, Li X, et al. Midterm results of diagnostic treatment and repair strategy in older patients presenting with non-restrictive ventricular septal defect and severe pulmonary artery hypertension. *Chin Med J* 2014; 127: 839–844.
- Sysol JR, Chen J, Singla S, et al. ID: 123: role of microRNA-1 in regulating pulmonary vascular remodeling in pulmonary arterial hypertension. *J Investig Med* 2016; 64: 969.
- Thompson AAR and Lawrie A. Targeting vascular remodeling to treat pulmonary arterial hypertension. *Trends Mol Med* 2017; 23: 31–45.
- Li N, Long B, Han W, et al. microRNAs: important regulators of stem cells. *Stem Cell Res Ther* 2017; 8: 110.
- Shantikumar S, Caporali A and Emanuelli C. Role of microRNAs in diabetes and its cardiovascular complications. *Cardiovas Res* 2012; 93: 583–593.
- Gupta S and Li L. Modulation of miRNAs in pulmonary hypertension. *Int J Hypertens* 2015; 2015: 169069.
- Mohsenin V. The emerging role of microRNAs in hypoxia-induced pulmonary hypertension. *Sleep Breath* 2016; 20: 1059–1067.
- Liu G, Hao P, Xu J, et al. Upregulation of microRNA-17-5p contributes to hypoxia-induced proliferation in human pulmonary artery smooth muscle cells through modulation of p21 and PTEN. *Respir Res* 2018; 19: 200.
- Wang P, Xu J, Hou Z, et al. miRNA-34a promotes proliferation of human pulmonary artery smooth muscle cells by targeting PDGFRA. *Cell Prolif* 2016; 49: 484–493.
- Liu H, Tao Y, Chen M, et al. Upregulation of microRNA-214 contributes to the development of vascular remodeling in hypoxia-induced pulmonary hypertension via targeting CCNL2. *Sci Rep* 2016; 6: 24661.
- Xiao T, Xie L, Huang M, et al. Differential expression of microRNA in the lungs of rats with pulmonary arterial hypertension. *Mol Med Rep* 2017; 15: 591–596.
- Sharma S, Umar S, Potus F, et al. Apolipoprotein A-I mimetic peptide 4F rescues pulmonary hypertension by inducing microRNA-193-3p. *Circulation* 2014; 130: 776–785.
- Liu A, Liu Y, Li B, et al. Role of miR-223-3p in pulmonary arterial hypertension via targeting ITGB3 in the ECM pathway. *Cell Prolif* 2019; 52: e12550.
- Livak KJ and Schmittgen TD. Analysis of relative gene expression data using real-time quantitative PCR and the 2(-Delta Delta C(T)) method. *Methods* 2001; 25: 402–408.
- Liu Y, Xiao H, Tian Y, et al. The pak4 protein kinase plays a key role in cell survival and tumorigenesis in athymic mice. *Mol Cancer Res* 2008; 6: 1215–1224.
- Thillai K, Sarker D and Wells C. PAK4 pathway as a potential therapeutic target in pancreatic cancer. *Future Oncol* 2018; 14: 579–582.
- Costa TDF, Zhuang T, Lorent J, et al. PAK4 suppresses RELB to prevent senescence-like growth arrest in breast cancer. *Nat Commun* 2019; 10: 3589.
- Zhang X, Zhang X, Li Y, et al. PAK4 regulates G6PD activity by p53 degradation involving colon cancer cell growth. *Cell Death Dis* 2017; 8: e2820.
- Jian B, Li Z, Xiao D, et al. Downregulation of microRNA-193-3p inhibits tumor proliferation migration and chemoresistance in human gastric cancer by regulating PTEN gene. *Tumour Biol* 2016; 37: 8941–8949.
- Nie X, Chen Y, Tan J, et al. MicroRNA-221-3p promotes pulmonary artery smooth muscle cells proliferation by targeting AXIN2 during pulmonary arterial hypertension. *Vascul Pharmacol* 2019; 116: 24–35.
- Mao K, Lei D, Zhang H, et al. MicroRNA-485 inhibits malignant biological behaviour of glioblastoma cells by directly targeting PAK4. *Int J Oncol* 2017; 51: 1521–1532.
- Lu X, Wang H, Su Z, et al. MicroRNA-342 inhibits the progression of glioma by directly targeting PAK4. *Oncol Rep* 2017; 38: 1240–1250.
- Meloche J, Pflieger A, Vaillancourt M, et al. miRNAs in PAH: biomarker, therapeutic target or both? *Drug Discov Today* 2014; 19: 1264–1269.
- Tang BI, Tang MM, Xu QM, et al. MicroRNA-143-5p modulates pulmonary artery smooth muscle cells functions in hypoxic pulmonary hypertension through targeting HIF-1alpha. *J Biosci* 2020; 45: 37.
- Zhao TF, Wang SY, Zou XZ, et al. MiR-593-5p promotes the development of hypoxic-induced pulmonary hypertension via targeting PLK1. *Eur Rev Med Pharmacol Sci* 2019; 23: 3495–3502.
- Yue Y, Zhang Z, Zhang L, et al. miR-143 and miR-145 promote hypoxia-induced proliferation and migration of pulmonary arterial smooth muscle cells through regulating ABCA1 expression. *Cardiovascular Pathol* 2018; 37: 15–25.
- Karimian A, Ahmadi Y and Yousefi B. Multiple functions of p21 in cell cycle, apoptosis and transcriptional regulation after DNA damage. *DNA Repair* 2016; 42: 63–71.
- Altomare DA, Zhang L, Deng J, et al. GSK690693 delays tumor onset and progression in genetically defined mouse models expressing activated Akt. *Clin Cancer Res* 2010; 16: 486–496.
- Nekrasova T and Minden A. PAK4 is required for regulation of the cell-cycle regulatory protein p21, and for control of cell-cycle progression. *J Cell Biochem* 2011; 112: 1795–1806.
- Yuan L, Duan X, Dong J, et al. p21-activated kinase 4 promotes intimal hyperplasia and vascular smooth muscle cells proliferation during superficial femoral artery restenosis after angioplasty. *Biomed Res Int* 2017; 2017: 5296516.
- Xue J, Chen LZ, Li ZZ, et al. MicroRNA-433 inhibits cell proliferation in hepatocellular carcinoma by targeting p21 activated kinase (PAK4). *Mol Cell Biochem* 2015; 399: 77–86.
- Sun L, Lin P, Chen Y, et al. miR-182-3p/Myadm contribute to pulmonary artery hypertension vascular remodeling via a KLF4/p21-dependent mechanism. *Theranostics* 2020; 10: 5581–5599.